



estec

European Space Research
and Technology Centre
Keplerlaan 1
2201 AZ Noordwijk
The Netherlands
T +31 (0)71 565 6565
F +31 (0)71 565 6040
www.esa.int

EarthCARE instruments description

Prepared by A.Helière, K. Wallace, J. Pereira do Carmo, M.Eisinger, T.Wehr, A.Lefebvre
Edited by R. Koopman
Reference EC-TN-ESA-SYS-0891
Issue 1
Revision 0
Date of Issue 24/05/2017
Status Approved
Document Type TN
Distribution

APPROVAL

Title EarthCARE instruments description	
Issue Number 1	Revision Number 0
Authors: A.Helière, K. Wallace, J. Pereira do Carmo, M.Eisinger, T.Wehr, Editor: Rob Koopman	Date 24052017  <small>Digitally signed by Rob Koopman DN: cn=Rob Koopman, o=European Space Agency, ou=ESD, email=Rob.Koopman@esa.int, c=NL Date: 2017.06.02 15:01:31 +02'00'</small>
Approved By	Date of Approval
D. Maesli	 <small>Digitally signed by Dariusz Maesli DN: cn=Dariusz Maesli, ou=ESD, ou=ESD PPM, email=dmaesli@esa.int, c=PL, title=2017.06.02 15:48:51 +02'00'</small>
A. Lefebvre	

CHANGE LOG

Reason for change	Issue Nr.	Revision Number	Date
-------------------	-----------	-----------------	------

CHANGE RECORD

Issue Number 1	Revision Number 0		
Reason for change	Date	Pages	Paragraph(s)

DISTRIBUTION

Name/Organisational Unit



Table of contents:

1. INTRODUCTION.....4

2. MISSION AND SATELLITE CONFIGURATION 5

3. EARTHCARE PAYLOAD REQUIREMENTS AND CONFIGURATION 9

1.1 The ATmospheric LIDar (ATLID) 9

1.1.1 ATLID measurement principle and key performance parameters..... 9

1.1.2 ATLID Configuration 10

Transmitter and Emitter chain 12

Receiver chain..... 13

Mechanical and thermal units..... 14

1.1.3 Instrument performance and data products15

Instrument performance 15

Data Products..... 15

1.1.4 In-flight calibration..... 16

Radiometric calibration..... 16

Spectral calibration..... 16

Spatial calibration..... 16

1.2 The Broad-Band Radiometer (BBR).....17

1.2.1 BBR concept17

1.2.2 BBR instrument description17

1.2.3 Calibration / Validation..... 19

1.3 The Cloud Profiling Radar (CPR)..... 21

1.3.1 CPR measurement principle and key performance parameters..... 21

1.3.2 CPR configuration 22

1.4 The Multi Spectral Imager (MSI) 23

1.4.1 The MSI concept 23

1.4.2 TIR camera module description..... 24

1.4.3 VNS camera module description..... 25

1.4.4 Calibration / Validation..... 26

1.4.5 MSI reconfiguration..... 27

4. SUMMARY 28

1. INTRODUCTION

The Earth Explorer Core Missions are an element of the European Space Agency Earth Observation Envelope Programme. They are defined as major missions led by ESA to cover primary research objectives set out in the Living Planet Program. EarthCARE, the Earth Clouds Aerosols and Radiation Explorer¹, has been selected for implementation as the third Earth Explorer Core Mission and is being developed in cooperation with the Japan Aerospace Exploration Agency (JAXA) who provides one of the active instruments.

The EarthCARE mission basic objective is to improve the understanding of the cloud-aerosol-radiation interactions and Earth radiative balance, so that they can be modelled with better reliability in climate and in numerical weather prediction models. Specifically, the scientific objectives are:

- Observation of the vertical profiles of natural and anthropogenic aerosols on a global scale, their radiative properties and interaction with clouds;
- Observation of the vertical distributions of atmospheric liquid water and ice on a global scale, their transport by clouds and their radiative impact;
- Observation of cloud distribution ('cloud overlap'), cloud precipitation interactions and the characteristics of vertical motions within clouds;
- Retrieval of profiles of atmospheric radiative heating and cooling through the combination of the retrieved aerosol and cloud properties

In order to fulfill the above objectives, the EarthCARE mission will collect co-registered observations from a suite of four instruments located on a common platform. The Optical payload encompasses the European instruments and consists of an ATmospheric LIDar (ATLID), a Multi- Spectral Imager (MSI) and a BroadBand Radiometer (BBR). The fourth instrument, provided by JAXA, is a Cloud Profiling Radar (CPR). The two active instruments will provide vertical profiles of the atmosphere along the satellite nadir path. The two passive instruments will provide scene context information to support the active instruments data interpretation.

The instruments' data will be processed individually and synergistically (see Figure 1) to retrieve the vertical structure and horizontal distribution of cloud and aerosol fields, together with the outgoing radiation, over all climate zones.

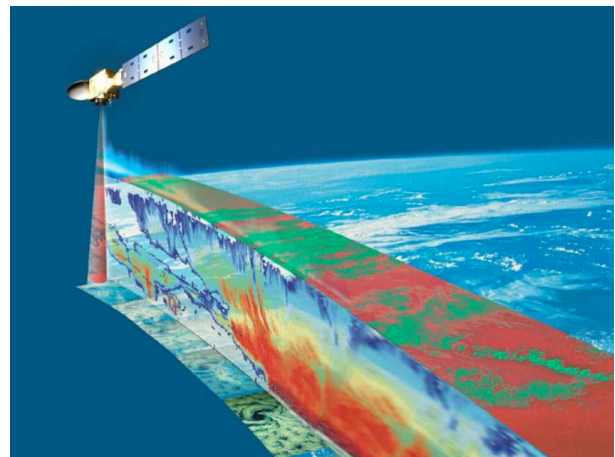
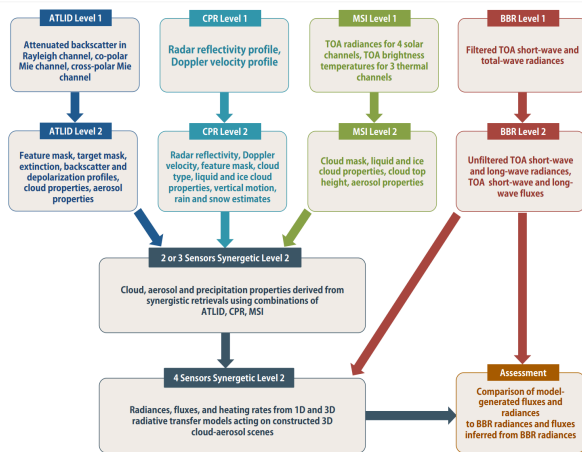


Figure 1: Contributions of multiple remote-sensing techniques to achievement of EarthCARE mission objectives

The Spacecraft Acceptance Review is planned not earlier than May 2019.

2. MISSION AND SATELLITE CONFIGURATION

Figure 1 provides an artist's view of the EarthCARE satellite in-orbit with both CPR antenna and solar array already deployed. The spacecraft configuration results from extensive trade-offs performed during the early phases of the Project. Optimization took place according to the major mission requirements, in particular the accommodation of the four instruments payload, their field of view, and the impacts of the relatively low orbit required to enhance the active instruments' performance. The streamlined shape of the spacecraft, with its trailing solar array, minimizes its cross-section and reduces the residual atmospheric drag.



Figure 2: EarthCARE artist view

The instrument viewing geometry in Figure 2 illustrates the satellite ground track, the CPR beam at normal nadir, the lidar beam depointed backward by 3° to reduce specular conditions, the across track swath of the MSI with its offset in the anti-sun direction to mitigate sun-glint and finally the 3 BBR views in nadir, forward and backward directions required to retrieve the emitted flux.

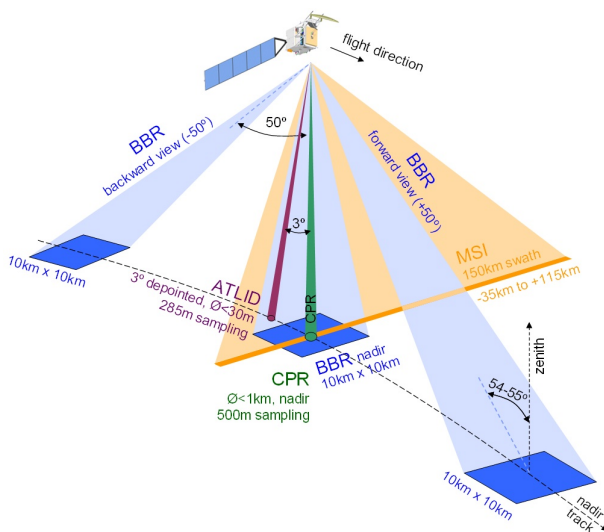


Figure 3: Instruments viewing geometry

Stringent platform and instrument alignment requirements are specified to ensure the co-registration of the two profiling active instruments measurements to better than 350m and accurate knowledge of their position in the swath of the imager. The spacecraft structure design, layout and materials have been selected for their good performance in this respect.

The achieved satellite cross-section in the flight direction leads to a very compact core spacecraft as shown of Figure 3, which is important due to the low orbit altitude. A semi-transparent view is presented here to allow visualizing the dense configuration of the platform and payload volumes and realizing the amount of engineering effort that the Airbus Defense and Space team has invested in the EarthCARE Satellite design. Once deployed in orbit, the overall spacecraft length is about 19 meters; the full solar array of 5 panels is not shown here.

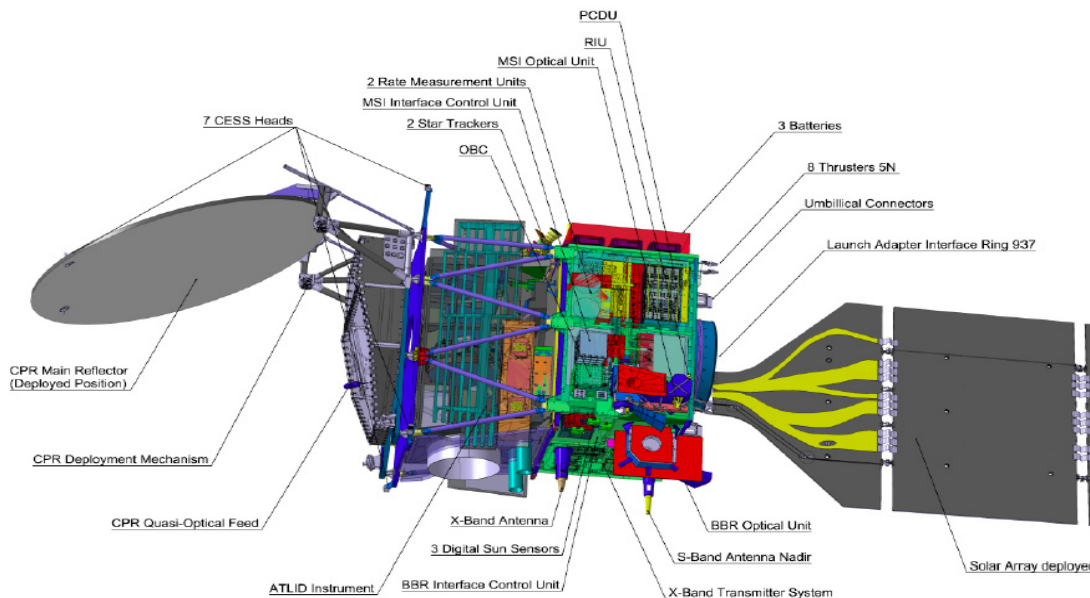


Figure 4: Spacecraft semi-transparent view

Overall the assembly of the satellite platform is well advanced as can be seen from Figure 4 below which shows the integrated spacecraft platform:



Figure 5: Integrated Spacecraft without payload

The baseline candidate for the launch vehicle is the Soyuz-CSG. EarthCARE is to be injected into a sun-synchronous near-polar orbit at an altitude of 393 km. The orbit has been selected to have a descending node crossing Mean Local Solar Time of 14:00 and a repeat cycle of 25 days. The orbit parameters can be summarised as follows:

Table 1: EarthCARE Orbit Parameters

<i>Parameter</i>	<i>Orbit Value (mean Kepler)</i>
Semi-major axis	$a = 6771.28 \text{ km}$
Eccentricity	$e = 0.001283$
Inclination (sun-synchronous)	$i = 97.050^\circ$
Argument of perigee	$\omega = 90^\circ$
Mean Local Solar Time, Descending Node	MLST = 14:00
Repeat cycle / cycle length	25 days, 389 orbits
Orbital duration	5552.7 s
Mean Spherical Altitude	393.14 km
Minimum Geodetic Altitude	398.4 km
Maximum Geodetic Altitude	426.0 km
Average Geodetic Altitude	408.3 km
Dead band	+/- 25 km nominal, +/- 1km limited (time & areas)

EarthCARE is designed for an in-orbit lifetime of three years but will carry sufficient consumables for a possible one-year extension of mission. The operational availability has been specified as 95% for the routine phase.

Once in orbit, the EarthCARE platform and its payload will interface to the EarthCARE ground segment for command & control and payload data processing. Schematically the ground segment will be implemented as in Figure 6. Mission

planning is performed at the ESA payload data ground segment (PDGS) with inputs from JAXA for the CPR. Command & control is performed at the ESA flight operations segment (FOS), and data processing and distribution at both ESA (ATLID, BBR, MSI level-1 and ESA level-2 products) and JAXA (CPR level-1b, and JAXA level-2 products). It should be noted that both JAXA and ESA produce some level-2 products involving input data from the other Agency.

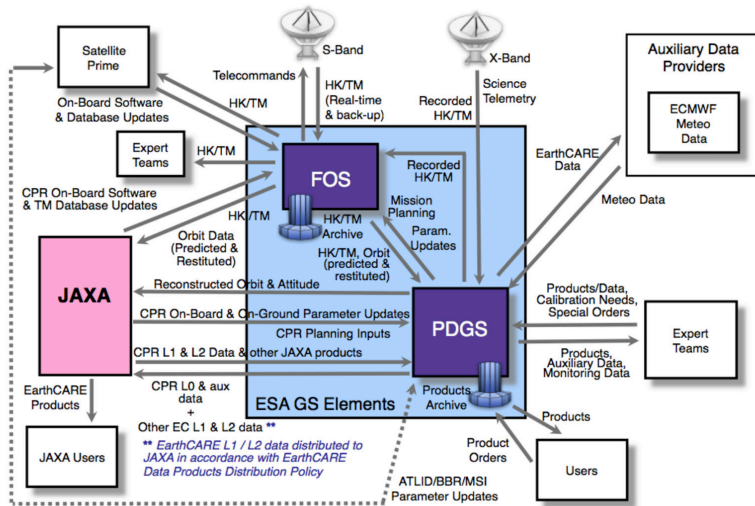


Figure 6: Layout of the EarthCARE ground segment and

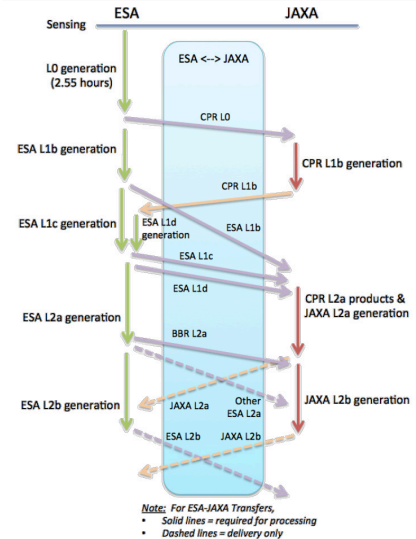


Figure 7: data exchanges between ESA and JAXA

In the payload data segments, a complex sequence of operations takes place to achieve the synergistic products.

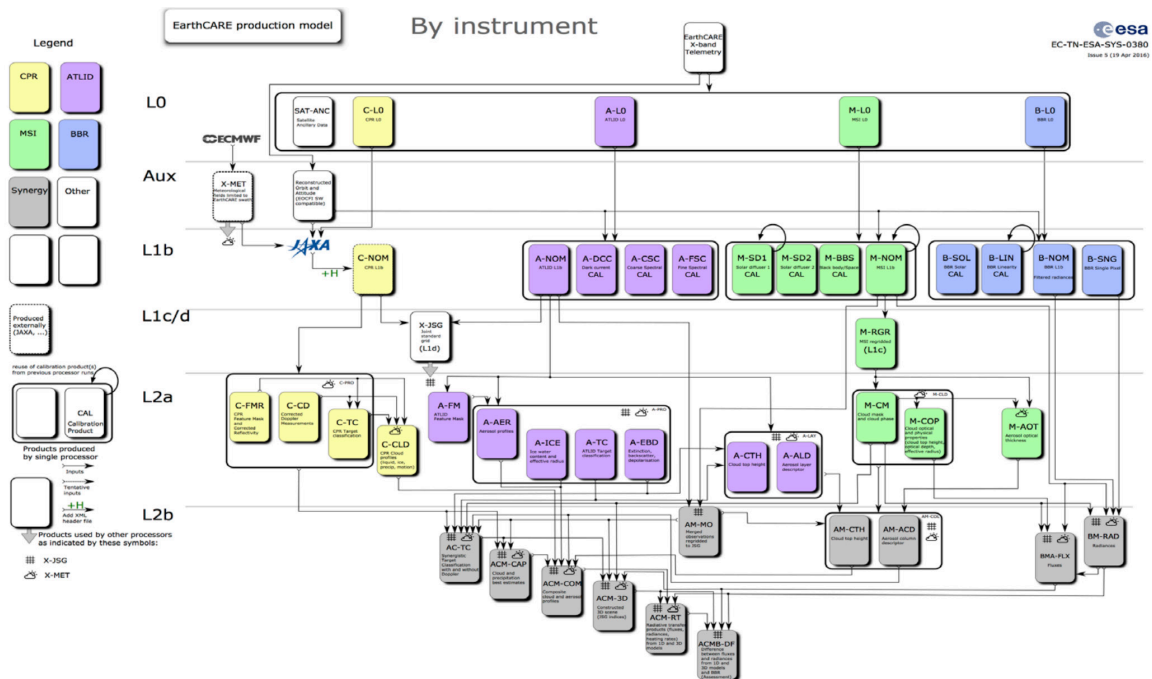


Figure 8: EarthCARE production model for the ESA products (using the JAXA CPR level 1b product as input)

3. EARTHCARE PAYLOAD REQUIREMENTS AND CONFIGURATION

The EarthCARE Payload is composed of new and challenging instruments and its development schedule has been lagging behind the Platform one. This has been specifically the case for the ATLID instrument whose development has been driven by the understanding of the issues of laser-induced damage (LID), laser-induced contamination (LIC) and mitigation approach. A change of instrument concept, from mono-static to bi-static has been identified and elaborated during the extended instrument Phase B. The new design, implemented as baseline at the start of the detailed design phase, has been fully consolidated in 2015.

Figure 4 describes the spacecraft configuration in stowed configuration and shows the four instruments location. Key instrument data is provided to highlight the demanding EarthCARE payload accommodation and budget requirements.

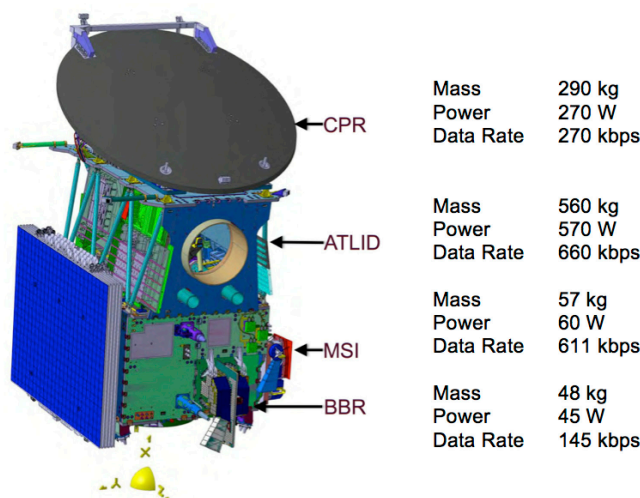


Figure 9: EarthCARE instruments accommodation and key instrument data

1.1 The ATmospheric LIDar (ATLID)

The objective of the ATLID instrument is to measure vertical profiles of optically thin cloud and aerosol layers.

1.1.1 ATLID measurement principle and key performance parameters

ATLID measures atmospheric profiles, in a direction close to the nadir (3 degrees shift along the satellite track), with a vertical resolution of about 100 m from ground to an altitude of 20 km and of 500 m from 20 km to 40 km altitude. The key performance parameters are indicated in table 1. The instrument transmitter emits short laser pulses with a repetition rate of 51 Hz -corresponding to about 140 m spatial resolution- along the horizontal track of the satellite so that several shots can be locally averaged to improve the signal to noise ratio. The ATLID receiver collects the backscattered photons with a ~ 60 cm diameter telescope. The UV pulses energy transmitted by the transmitter will be subject to narrow-band particle scattering from atmospheric aerosols, which do not affect the spectrum shape of the incident light, and Rayleigh scattering due to the Brownian motion of atmospheric molecules, which causes broadening of the incident spectrum.

Table 2: ATLID key performance parameters

Item	Specification			
Operating wavelength	354.8 nm			
Emitted energy	38 mJ			
Receiver footprint diameter	≤ 30 m			
PRF	51 Hz			
Transmit pulse width	20 ns			
Altitude range	-0.5 to +40 km			
Vertical sampling interval	100 m			
Along track sampling interval	285 m			
Dynamic range	10 ⁻⁷ to 9.61x10 ⁻³ sr ⁻¹ m ⁻¹			
Radiometric stability	1%			
Observation requirements		Mie co-polar channel	Rayleigh channel	Mie cross-polar channel
	Cirrus optical depth	0.05		
	Cirrus backscatter sr ⁻¹ m ⁻¹	8 10 ⁻⁷		2.6 10 ⁻⁵
	Vertical resolution	100 m	300 m	100 m
	Horizontal resolution	10 km		
	Required Accuracy	50%	15%	45%

After collection of the backscattered photons by its telescope, the receiver chain uses a high spectral-resolution etalon filter to separate the particle and Rayleigh components in order to retrieve the aerosol optical depth. Co- and cross-polarised components of the particle scattering contribution will also be separated and measured on dedicated channels to allow aerosol classification (see Figure 10 for the filtering approach).

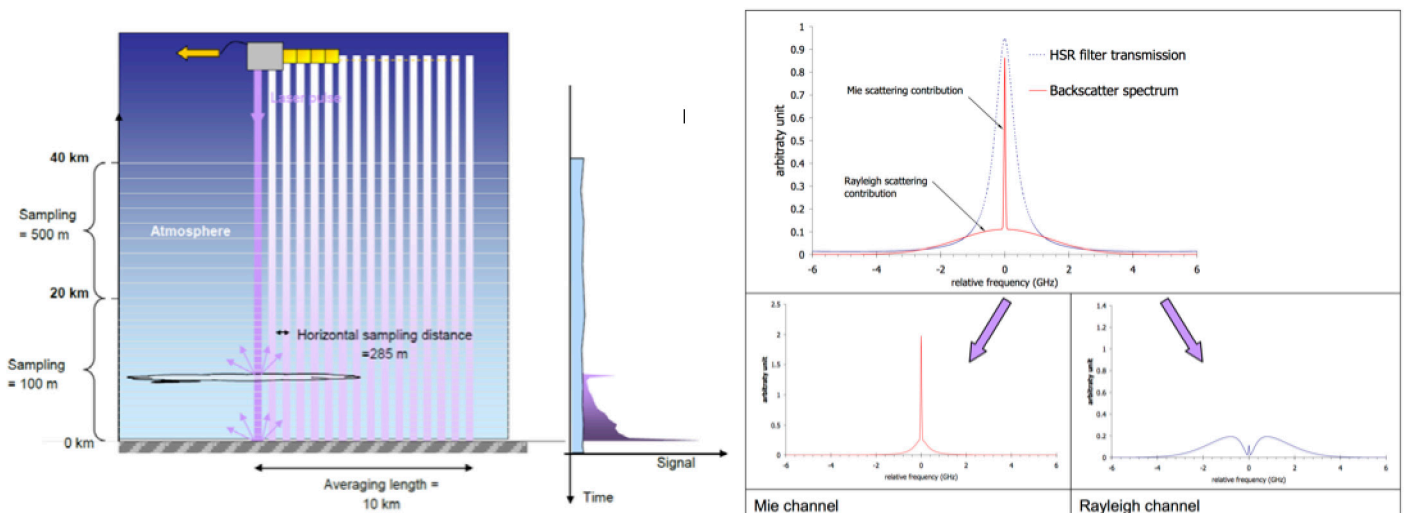


Figure 10: Instrument sampling and retrieval approach

1.1.2 ATLID Configuration

The ATLID configuration overview is shown in Figure 10. An external enclosure, the complex Housing Structure Assembly (HSA), accommodates all ATLID sub-systems and provides the instrument mechanical interfaces to the spacecraft. The HSA also supports all external radiators, the large telescope baffle and the instrument electronics units (mounted inside the HSA). The right part of the picture shows the instrument internal support bench, 'Stable Structure Assembly', accommodated with all alignment critical units and sub-systems. These include the redundant transmitters with their long baffles and the receiver chain from primary mirror to Focal Plane Assembly.

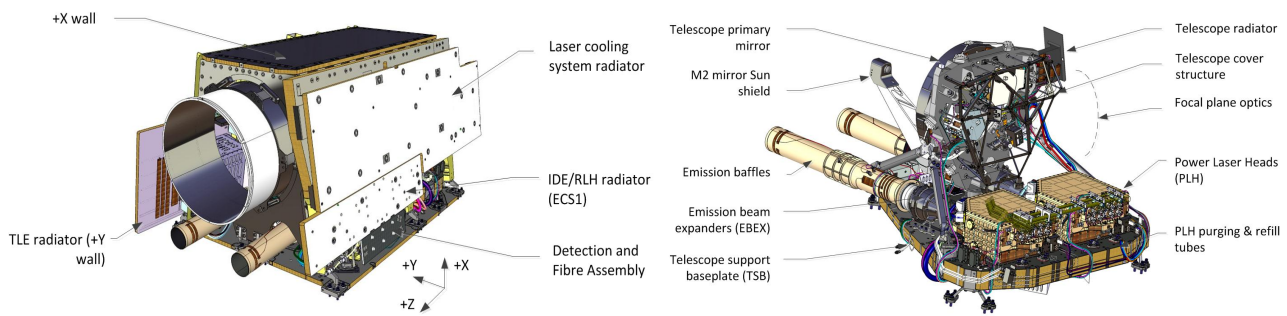


Figure 11: ATLID configuration overview and stable structure assembly accommodating both emission and receiver chains

The Emitter chain includes:

- The laser Transmitter Assembly, consisting of a Power Laser Head (PLH) and its Transmitter Laser Electronics, and a Reference Laser Head which provides the stable seed laser. The laser is a diode pumped single-mode laser emitting at 355 nm (tripled frequency of a Nd:YAG laser). It consists of a Master Oscillator section generating low pulse energy of about 8mJ, a Pump Unit amplifying the pulse energy to 135mJ and a harmonic conversion stage doubling, then tripling the laser frequency. The emitted polarisation is linear. The Reference Laser Head seeding the laser oscillator is used to meet the stringent frequency stability requirements. Its frequency is stepwise tuneable to allow frequency scan operations for calibration purposes. The Laser Head includes also a Beam-Steering Mechanism finely adjusting the emission line-of-sight to continuously maintain emission / reception co-alignment in flight, based on information acquired in reception chain by a Co-Alignment Sensor. The laser transmitter is a key driver to the instrument budgets with a power consumption of 300 W, cooled down by a set of mini loop heat pipes. It delivers pulses of more than 38 mJ UV energy with duration of about 25 ns at a pulse repetition frequency of 51Hz. The laser transmitter has also stringent spectral requirements with a spectral linewidth below 50 MHz and a 25 GHz spectral tuneability range.
- The Emission Beam Expander (E-BEX), used to enlarge laser beam at Power Laser Head output in order to meet the divergence requirement (beam diffraction is reduced by increasing the emitted beam diameter) and to minimise the laser fluence on last dioptré exposed to vacuum. The reduction of fluence allows on one side increasing margin with respect to damage threshold, but is particularly needed to mitigate Laser Induced Contamination (LIC) effect, which darkens optical surfaces when contaminated dioptrés are exposed to UV light in vacuum. The E-BEX is sealed and pressurised to avoid LIC effect on its internal surfaces due to presence of oxygen. The E-BEX temperature can be adjusted in order to finely tune the defocus; this function allows minimising emission divergence by in-flight refocus of laser beam in case of PLH focus evolution or E-BEX internal pressure variation leading to defocus. The E-BEX can also be heated up to 40°C during non-operational phases in decontamination mode..
- The emission baffle: this baffle aims at protecting the EBEX output window from external contamination during instrument and satellite assembly and test, and during flight.

The Receiver chain includes:

- The receiver telescope: it is an afocal Cassegrain with 620mm primary mirror diameter aiming at collecting the backscattered light. It is made of Silicon Carbide to ensure high stability.
- Receiver optics: this goes from telescope output to detector fibres entrance. It comprises the entrance filtering optics (narrow interference filter with less than 1 nm bandwidth), the blocking filtering optics (spatial filtering with a field-stop delimiting the 65 μ rad field-of-view), and the High Spectral Resolution filter based on Fabry-Perot etalon. The signal is transported to the detectors by means of fibre couplers, allowing deporting the whole detection chain on the anti-sun wall for passive cooling. Part of the flux is split at focal plane assembly entrance and imaged on the Co-Alignment Sensor which provides laser spot position information.
- The science channels detection functions: they are ensured by the Memory CCD and the Instrument Detection Electronics. The detection chain shall be able to measure single photon events to meet the worst case radiometric performance requirements. The selected design provides high response together with an extremely low noise thanks to on-chip storage of the echo samples which allows delayed read-out at very low pixel frequency (typically below 50 kHz). Combined with an innovative read-out stage and sampling technique, the detection chain provides an extremely

low read-out noise ($< 2e^-$ RMS per sample). The detection electronics are also responsible for the management and video processing of the Co-Alignment Sensor.

- The control and data management unit: including its own software in order to provide full autonomy in operation management, it ensures the synchronisation between laser emission and backscatter signal acquisition, the data processing and data stretching toward the spacecraft, the thermal regulation functions, the co-alignment control loop software (including co-alignment sensor images processing and centroiding algorithms) as well as the beam steering mechanism commanding, the TM/TC and observability management.

Transmitter and Emitter chain

While the laser transmitter is largely inheriting from the Aladin instrument development for the AEOLUS mission, a significant evolution of the laser design lies in the fact that ATLID power laser head is sealed and pressurized. This improvement ensures more stable operating conditions to the sensitive components of the laser, and isolates the laser internal space from surrounding contaminants over the ground and operational lifetime. Pressure also improves tolerance to laser induced contamination, which is the degradation of an optical surface resulting from the interaction of molecular contamination with a high laser illumination level. The mechanical design is based on a double-sided aluminium bench interfaced to ATLID support baseplate via 3 iso-static mounts. The “H” architecture of the bench ensures that bench distortion due to pressurisation is minimised.

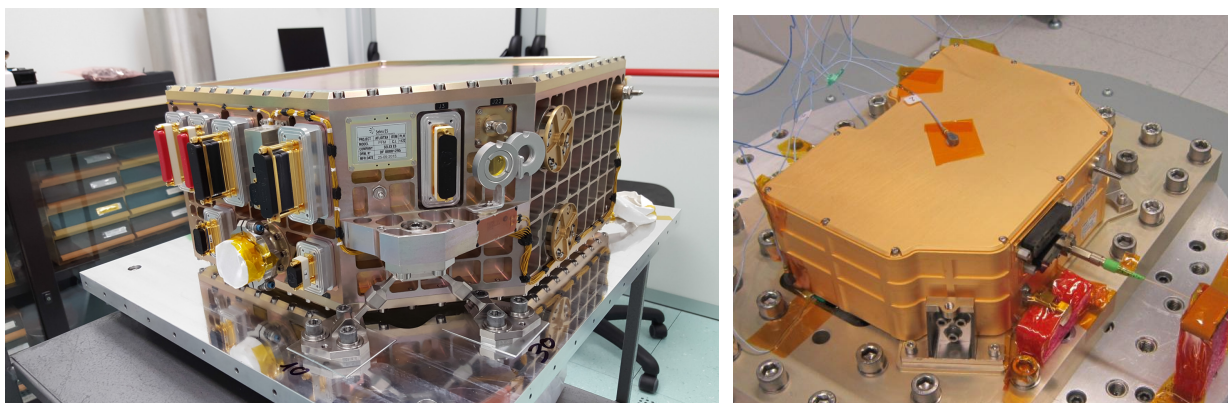


Figure 12: Power Laser Head and Reference Laser Head Flight Models

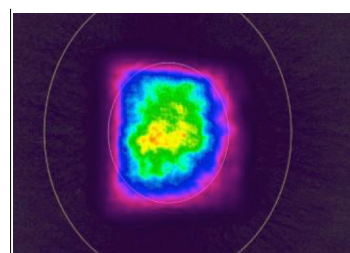


Figure 13:– Typical UV beam Near field distribution

ATLID is equipped with 2 full transmitter chains implemented in cold redundancy.

The Beam Steering Assembly consists in a Beam Steering Mechanism integrated into the Power Laser Head and its control electronics.

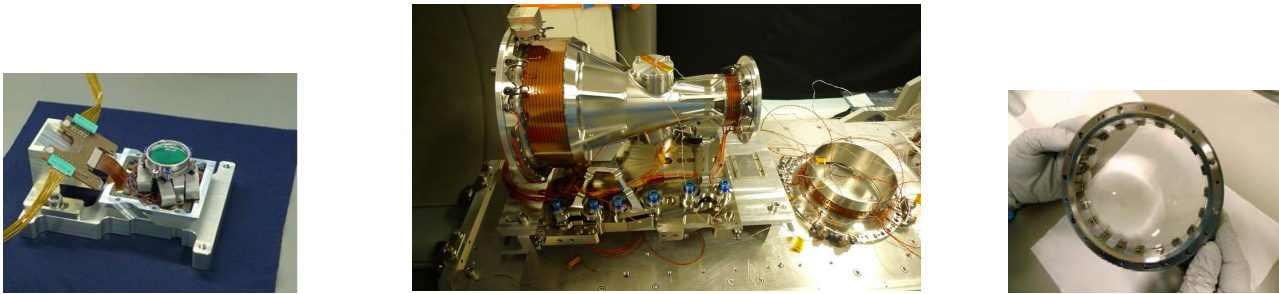


Figure 14: Beam Steering Mechanism Qualification Model- Emission Beam Expander PFM body and lens.

The Emission Beam Expander is sealed and pressurised with dry air and shall expand the laser beam to more than 100mm diameter: this requires large brazed windows, large lense mounts development with stringent requirements in WFE, high transmission and qualification for laser irradiation.

Receiver chain

The receiver chain includes a silicon carbide telescope of excellent image quality performance with wave front error in the range of 40nm rms. The chain also includes the Entrance Filtering Optics (polarisation control and narrow bandpass interference filter) and the Blocking Filter (spatial filtering).



Figure 15: ATLID receiving telescope- Blocking Filter and Entrance filter units.

A key unit of the ATLID instrument is the High Spectral Resolution Etalon used in the receiver to split the collected backscatter signal into 3 channels aimed at detecting the Rayleigh backscatter, the Mie backscatter co-polar and cross-polar signals. This unit is made of a narrow bandwidth Fabry-Perot etalon combined with a set of prisms. The etalon is subject of very challenging requirements (only a few nanometers parallelism are tolerated over a 40 mm distance).

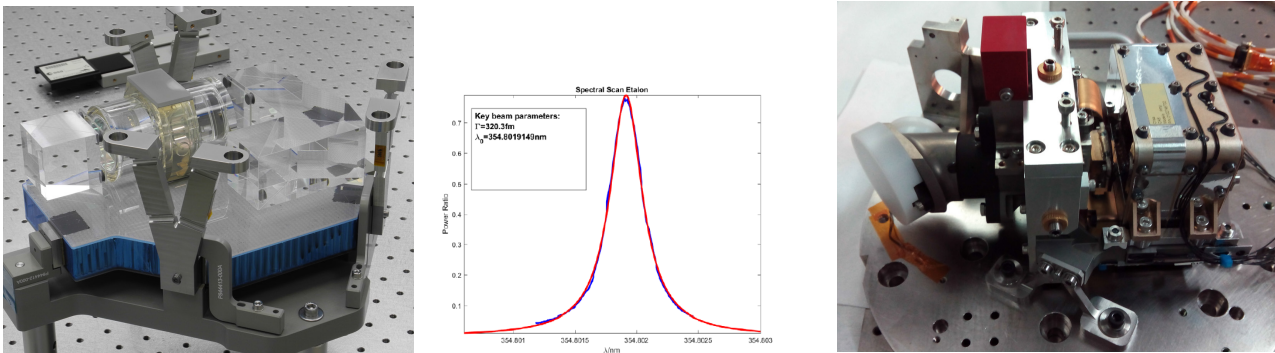


Figure 16: PFM High Spectral Resolution Etalon and typical spectral transmission – PFM Co-alignment Sensor

The Fibre Coupler Assemblies collect the signal from the telescope focal plane to the detectors. The Co-Alignment Sensor (CAS) is aiming at measuring the retro-reflected laser spot with better than 1/10 pixel accuracy.

Mechanical and thermal units

Due to the large number of units, the strong dissipation induced by the laser transmitter, and the interface on carbon fibre panel, ATLID mechanical and thermal implementation is particularly complex. One single interface panel supports all functions of the ATLID instrument, building a full ‘self standing’ instrument. The ‘high stability’ assembly (telescope, lasers, presented in Figure 10), electronic equipments and detection, harness and thermal hardware are mounted on this panel, directly or via secondary structures.

Stability performance is favoured by the assembly of laser and optics on a single carbon fibre sandwich base-plate, from which all units out of the stability chain are excluded. This sandwich structure allows optimizing both high stiffness for supporting both 37kg laser units and low hygro-thermal expansion for stability.



Figure 17: PFM Stable Structure Assembly integrated with long emitter baffles– PFM Housing Structure Assembly

The large dissipation (above 600 W) of the units together with the inhomogeneity of materials (aluminium for electronics, carbon-fibre for interface panel) requires for the housing structure assembly a complex assembly of aluminium sandwiches, aluminium structure, titanium blades and brackets, and carbon-fibre panel.

1.1.3 Instrument performance and data products

The mission requirements are specifying that the instrument shall detect thin clouds and aerosols with an extinction coefficient as low as 0.05 km^{-1} and very faint backscatter signal level of $8 \cdot 10^{-7} \text{ m}^{-1} \cdot \text{sr}^{-1}$, this with a vertical resolution lower than 300 m and horizontal integration lower than 10 km. Reference atmospheric scenes were defined at an early stage of the programme to perform the sizing of the instrument. Typically, thin cirrus extending from 9 to 10 kilometres altitude above a dense cloud located at 4 km altitude were considered, as shown in Figure 1.12.

Figure 18: ATLID reference atmospheric scenario

Instrument performance

The sensitivity of the Rayleigh channel is such that accurate measurements of aerosols and cirrus optical thicknesses as low as 0.05 can be performed. Furthermore, the depolarisation channel must be able to determine cirrus clouds having a backscatter signal of $2.6 \cdot 10^{-5} \text{ m}^{-1} \cdot \text{sr}^{-1}$ and 10 % depolarization ratio. Table 1 summarizes the main requirements for the observation of ATLID.

	Mie co-polar channel	Rayleigh channel	Mie cross-polar channel
Cirrus optical depth	0.05		
Cirrus backscatter $\text{sr}^{-1} \text{ m}^{-1}$	$8 \cdot 10^{-7}$		$2.6 \cdot 10^{-5}$
Vertical resolution	100 m	300 m	100 m
Horizontal resolution	10 km		
Required Accuracy	50%	15%	45%

Table 3: Radiometric accuracy specified for the 3 science channels

Additionally ATLID will perform measurements with a linearity error lower than 3%, as well as ensuring a radiometric stability of the order of 1%. The instrument also provides an in-flight calibration of the absolute channel response for the Mie and Rayleigh channels better than 10 %.

Numerical models and atmospheric models, including clouds and aerosols models, have been developed to evaluate the performance instrument. The performance estimates take into account the stringent satellite pointing requirements and instrument calibration accuracy.

Data Products

Instrument performance is specified by the level 1b data products. Level 1b products are the attenuated backscatter signals of the Rayleigh, Mie and depolarization (co-polarisation and cross-polarisation) channels from 0 to 40 km altitude. Products must be fully geo-localized.

Level 2 data products are geophysical products retrieved from Level 1b data plus auxiliary data, such as meteorological data. Level 2a products consist of:

- feature mask and target classification
- extinction, backscatter and depolarisation profiles
- aerosol properties
- ice cloud properties

Level 2b data products are geophysical parameters retrieved from the synergistic exploitation of two or more instruments. The ‘synergistic products’ consist of target classification, cloud and precipitation best estimates, vertical motion within clouds, cloud top height, cloud fraction, overlap and averaged microphysics, aerosol column descriptor, 3D cloud and aerosol scenes and radiative properties products.

1.1.4 In-flight calibration

The in-flight calibration enhances the most important calibration parameters and also corrects instrument drifts.

Radiometric calibration

The radiometric calibration is carried out during the normal measurement flow. The calibration parameters are extracted by proper selection of echoes and post processing. The main calibration sequences are:

- Earth background light is estimated before and after each echo, which allows an accurate offset subtraction on each echo.
- The spectral and polarisation cross-talks are continuously monitored by applying a dedicated processing on stratospheric backscatter (assuming containing pure Rayleigh backscatter) and cloud/ground echoes.
- The lidar constants of each channel are calibrated using the atmosphere backscatter (stratosphere and ground echoes) in conjunction with backscatter prediction model and selected test site with known ground albedo and atmosphere optical depth.
- Provision is made for regular detection dark signal calibration for potential compensation of dark signal non-uniformity, even if the low operation temperature of detector (-30°C) makes this offset theoretically negligible.

Spectral calibration

The instrument is able to perform spectral calibration in-flight thanks to the laser tunability capability around the emitted wavelength. The frequency calibration approach that is retained for ATLID consists of a laser frequency scan around the etalon central frequency. After launch, a coarse spectral co-registration sequence is necessary to tune the laser frequency around the receiver peak frequency. The sequence consists in sweeping the laser frequency over its tunability range (-12 / +12 GHz), and continuously record the atmospheric echoes. The atmospheric echo is acquired with the same operation sequence as nominal measurement. Ground or strong cloud echoes are extracted from measurements to derive the maximum receiver response where the laser frequency match the receiver filtering response. Additionally, fine spectral calibration of the laser is regularly performed to compensate for laser frequency drifts and other detuning contributors (filters, pointing, etc.). The same method used as for the coarse spectral calibration is used, and the relative calibration constant called spectral cross-talk, which is equal to (signal on Rayleigh channel) / (signal on Mie channel), is calculated from these echoes.

The receiver has also a limited spectral tunability capability by thermal tuning of the solar background rejection filter made of a Fabry-Perot etalon. This is used only for initial response optimisation after launch.

Spatial calibration

The instrument has two spatial calibrations capabilities. The first one is aimed at ensuring that the laser beam is always co-aligned to the receiver field of view. As the instrument is based on a bistatic configuration, the receiver and emitter have separate line of sights. This spatial alignment capability is compensating for potential in-orbit mis-alignment due to

thermo-elastic instabilities over the orbit and also for gravity release, units and telescope setting, moisture release that will occur after launch.

While a coarse co-alignment is performed after launch over a larger angular range, only minor correction are expected in the routine in-orbit operations.

The second spatial calibration consists in correction of the focussing/divergence of the laser spot to ensure the backscatter signal from the atmosphere is fully collected within the receiver field of view. This calibration is performed by thermal tuning of the Emission Beam Expander, adjusting the emitted beam focussing and acquiring laser return spot on the Co-Alignment Sensor. The on-ground analysis of these images allows retrieving the laser divergence and identifying the “best focus” set point. The update temperature command is then uploaded to the instrument.

1.2 The Broad-Band Radiometer (BBR)

1.2.1 BBR concept

BBR provides an estimate of the outgoing solar reflected and earth emitted thermal fluxes for a 10 km scene. The 34 kg Optics Unit (OU) will measure the top of atmosphere (TOA) radiance, at the same location, in two wavebands, using three quasi-simultaneous along track views that point nadir, forward and aft of nadir. BBR performs measurements in a Total Wave (TW) and a Short Wave (SW) band and provides top of atmosphere radiance data. Long Wave (LW) data is estimated by subtraction of SW from TW channel measurements. Measured radiance is filtered by the instrument spectral response. After un-filtering, using correlation with MSI data for improved performance, an estimate of the reflected solar and Earth emitted radiances will be obtained. Conversion to flux is performed analytically using Angular Dependence Models. The BBR radiances and derived fluxes can be compared to radiances and fluxes modelled from cloud and aerosol profiles synergistically retrieved from ATLID, CPR and MSI observations. By this, the BBR observations serve as an assessment of the retrieved cloud and aerosol scenes.

The BBR comprises the 34 kg OU and a 10 kg ICU. The BBR instrument development is undertaken by TAS-UK, in collaboration with RAL Space, which is developing the OU and ESTL, which is developing the mechanisms. TAS-UK is responsible for all three European ICUs and SSL is developing the software.

1.2.2 BBR instrument description

SW channel	< 0.25 to 4.0 μm
TW channel	< 0.25 to > 50 μm
Angular sampling (observation-zenith angle)	0, +55 and -55 $^\circ$
Spatial resolution	10 x 10 km
Spatial sampling distance	1 km
Dynamic range SW	0 to 450 $\text{W m}^{-2} \text{sr}^{-1}$
Dynamic range TW	0 to 550 $\text{W m}^{-2} \text{sr}^{-1}$
SW radiometric accuracy	2.5 $\text{W m}^{-2} \text{sr}^{-1}$
LW radiometric accuracy	1.5 $\text{W m}^{-2} \text{sr}^{-1}$
Radiometric stability	0.5 % both channels

Table 4. Key performance parameters of the BBR.

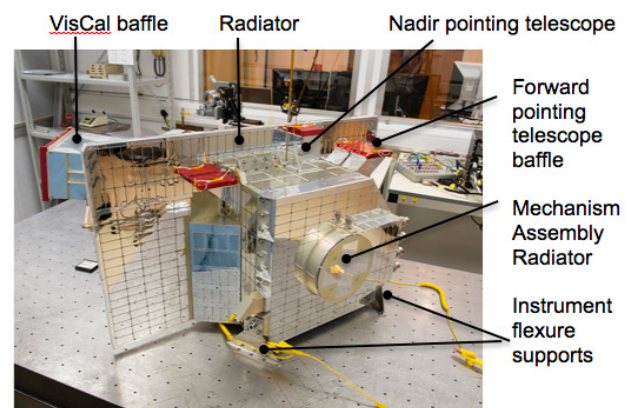


Figure 19. BBR flight model, with covers on.

Three identical, fixed mirror, dedicated telescopes image each of the fore, nadir and aft views onto linear array detectors. The pixel responses are given a near triangular shape by introducing a deliberate de-focus of each telescope. This is in order to give uniform system-PSF, achieved by summing of pixels, and to minimise the effects of diffraction. Less defocus is applied to the oblique view telescopes, in order to avoid loss of spectral resolution at the increased ranges. The detectors used are linear, 30 pixel, micro bolometer arrays from the Canadian institute, INO, to which a special gold-black coating has been applied to the 0.1x0.1 mm pixels in order to increase their sensitivity to TIR. BBR's radiator is located approximately mid of the Optics Unit. The telescopes are mounted onto a baseplate that is parallel to that radiator.

A chopper drum with four apertures - two of which house 2 mm thick, curved, quartz filters - rotates continuously around the telescopes, chopping the signal onto the detectors through SW/ drum skin/ TW/ etc.; the chopping scheme is based on GERB heritage. The drift dimension during detector integration is much smaller than the detector footprint. The nominal duration of each measurement view, 19 ms, is not long enough for the detector to reach a stable voltage and the digitized waveform of the measured view is processed to predict the asymptote of the exponential rise in the detected signal. The chopper drum speed is programmable and a flexible speed control has been implemented in order to optimise mechanism lifetime. Chopper drum speeds from 1x to 0.5x nominal can now be commanded. During In-Orbit Verification a sequence of tests will be performed in order to decide on a scenario for the Exploitation Phase.

Around the Chopper Drum sits the Calibration Target Drum, which houses hot and cold blackbodies, a diffusor, three fold mirrors to view the diffusor from each telescope, and the telescope baffles. The Chopper Drum and Calibration Target Drum mechanisms are nested and located at the opposite side to the Telescope Assembly baseplate. Both mechanisms operate on dry-lubricated bearings, the chopper bearing with a PGM-HT cage and the calibration bearing with a lead bronze cage.

Separate mounted boxes are located on the opposite side of the radiator and house the Signal Conditioning Electronics and the Visible Calibration (VisCal) system. The VisCal system houses a complex arrangement of mirrors, internal baffling and an external illumination baffle, that directs solar illumination onto the Calibration Target Drum mounted diffusor. Although the VisCal is not visible in Figures 15 and 16, its baffle can be seen.

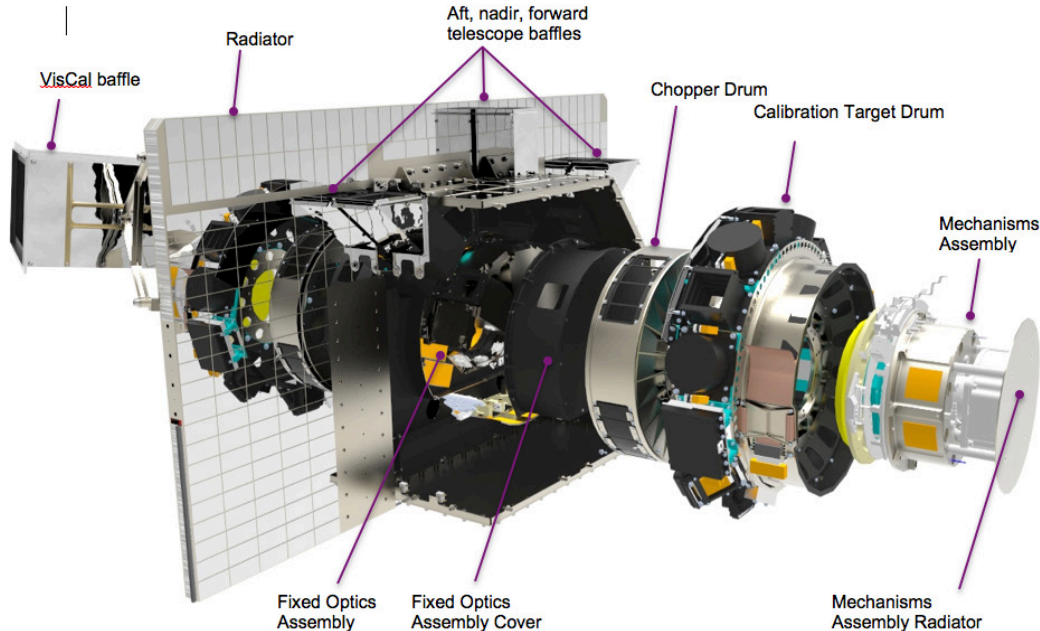


Figure 20. Exploded view of the BBR

The BBR will perform sampling such that the views from each of the three observation angles are spatially coincident, slightly separated in time. This requires the instrument to accommodate the residual shifts in scene position of the three fields of view that arise from Earth rotation between measurements after the implementation of yaw steering. For each telescope view a 10 x 10 km scene Point Spread Functions (PSF) is synthesised by summation of individual pixel PSF

responses along and across track. Pixels are selected to form scenes at 1 km intervals along track. To reduce the effect of overlapping radiances (from pixels outside of the nominal footprint) the PSF of edge pixels are weighted accordingly. The match of the scenes, for the two channels and the three view directions, is controlled by the Integrated Energy requirements.

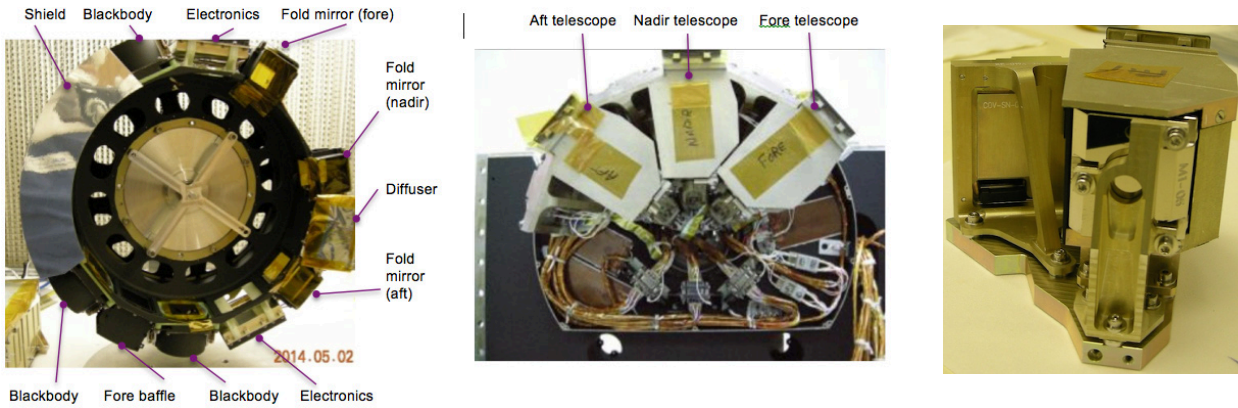


Figure 21. Calibration Drum (left), Telescope Baseplate Assembly (centre) and individual telescope (right). The nadir and aft baffles and one blackbody are hidden behind the shield on the Calibration Drum.

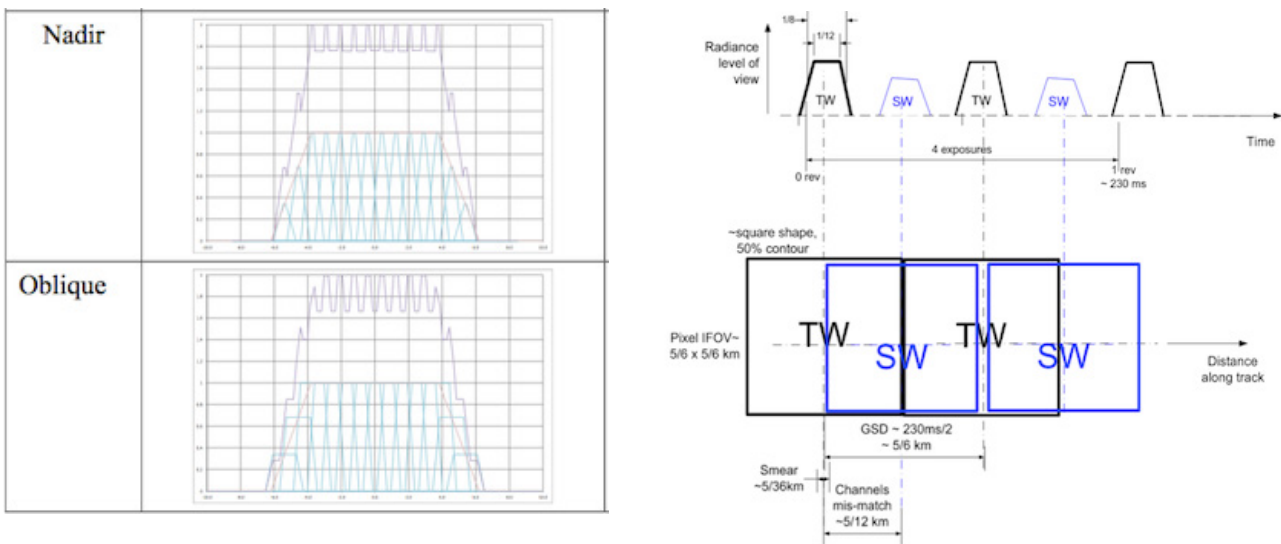


Figure 22. Scene formation by a telescope of the BBR. Alternate views of the SW and TW are exposed. The 10 km scene is synthesised via addition of single pixel PSFs that are weighted at the edges in order control the co-registration of the views and meet the integrated energy requirements. The chopper rotation speed in this diagram is nominal.

1.2.3 Calibration / Validation

LW calibration: Gain and offsets in the measured voltage signals are removed using hot and cold blackbodies that are autonomously rotated into the field of view every 88 s. This calibration frequency is decided by the temperature stability of the Chopper Drum skin and can be modified, if necessary, on orbit. The four instrument blackbodies are operated in hot redundancy and have been characterised on ground against an NPL BB that is traceable to radiometric standards. Every six months on-orbit the blackbody temperatures are swapped, allowing a check on instrument linearity by recording data over a range of radiance.

SW calibration: LW gain is transferable to the SW, with knowledge of the filter spectral response that is measured on ground. SW gain is monitored in-flight via measurements made with the VisCal system, to detect changes in instrument

response due to, for example, aging. The wall of each telescope baffle incorporates a set of three Monitor Photo Diodes, in order to monitor in turn aging of the VisCal optical path. The solar calibration is performed over approximately 30 orbits every two months and occurs in conjunction with the MSI solar calibration, in order to maximise mission availability.

The PSF of the pixels in the microbolometer arrays are also characterised on-ground, in order to formulate the algorithm for summing pixels to form the 10 km synthesised scene-PSF.

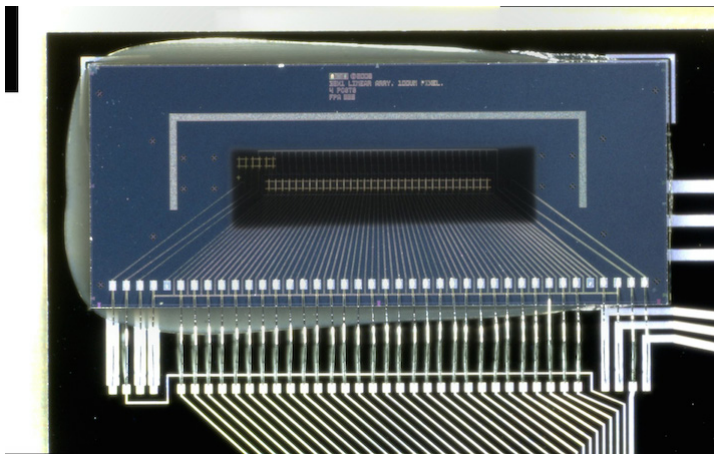


Figure 23. FM2 microbolometer FPA, post acceptance tests. The gold black coating is laser etched around each of the array pixels. The FPA is mounted on a silicon carrier chip, onto which is also fixed the read out circuit (ROIC). Connections between FPA and ROIC are achieved via wire bonds to the carrier chip. The carrier chip is in turn connected electrically via wire bonds to the circuit card.



Figure 24. Flight Mechanisms Assembly. The assembly is standing on the radiator and wiring to the chopper mechanism encoder is visible in the bottom section. At the top of image the circuit cards of the calibration mechanism encoder are visible. The discs at top of image interface to calibration and chopper drums.

Detector Point Spread Functions (PSFs) were measured at telescope level at Imperial College London. Pixel level PSF shape is used in the derivation of the summing algorithm that is used to shape the scene PSF.

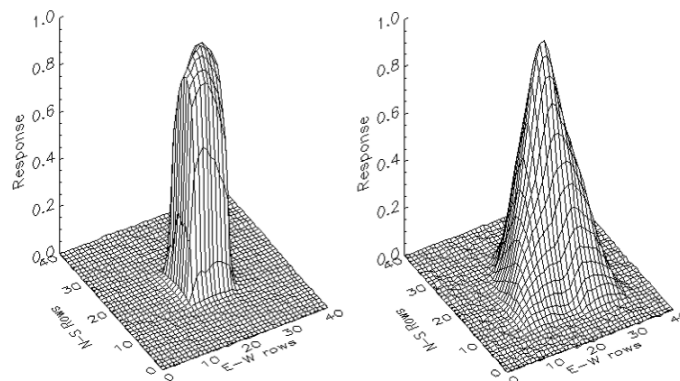


Figure 25. Response of pixel 15 (left) and pixel 0 (right)

The thermometers of the instrument blackbodies (IBBs) have been calibrated using an NPL calibrated blackbody. The IBB calibration will be carried out during the instrument calibration in thermal vacuum.

1.3 The Cloud Profiling Radar (CPR)

The objective of the CPR is to measure the vertical structure of clouds along the satellite track for the retrieval of their microscopic and macroscopic properties, and for the measurement of the vertical velocity of cloud particles. The instrument development is under the responsibility JAXA in Japan.

1.3.1 CPR measurement principle and key performance parameters

The CPR is a high power 94 GHz radar that measures the vertical profiles of clouds along the sub-satellite track. It emits microwave pulses at variable repeat frequency, which penetrate deep into lower cloud layers that are not visible for optical instruments.

The lowest measurement altitude extends to - 1 km in order to permit the use of surface backscatter, and the highest measurement altitude is ~ 20 km. Vertical sampling interval is 100 m. The instrument measurement principle and its main performance parameters are shown in Figure 6.

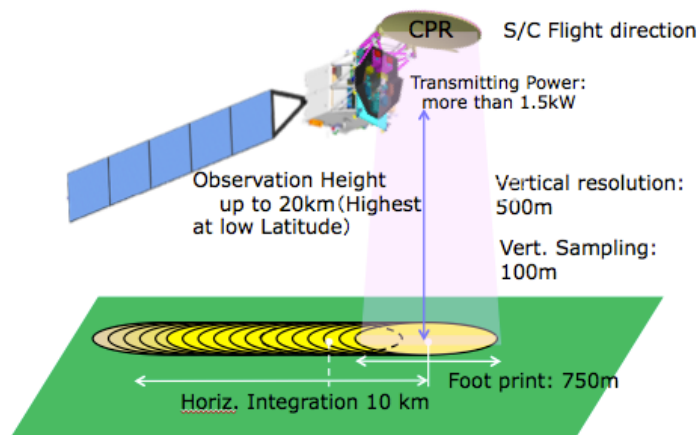


Figure 26: CPR Measurement principle

Parameter	Value
Centre frequency	94.05 GHz
Pulse width	3.3 μ s
Polarisation	Circular
Transmit power	> 1.5
Height range	Up to 20km (highest at low Latitude)
Vertical resolution	500 m (100m sampling)
Horizontal resolution	750 m (antenna footprint)
Minimum sensitivity	-35 dB
Pulse repetition frequency	Variable in range 6100 to 7500 Hz
Beam width	0.095 degree
Antenna aperture diameter	2.5 metre
Pointing accuracy	< 0.015 degree
Doppler range	\pm 10 m/s
Doppler accuracy	1 m/s

Table 4: Performance requirements as defined in the EarthCARE System Requirements Document (EC-RS-ESA-SY-0001 v1A)

1.3.2 CPR configuration

The CPR configurations on the spacecraft, stowed and deployed, are shown in Figure 7. The reflector size of 2.5 m aperture diameter is derived from the Radar performance requirements (sensitivity, Doppler, Field of view). All the radar active sub-systems are enclosed within the arrow-shape platform visible under the antenna.

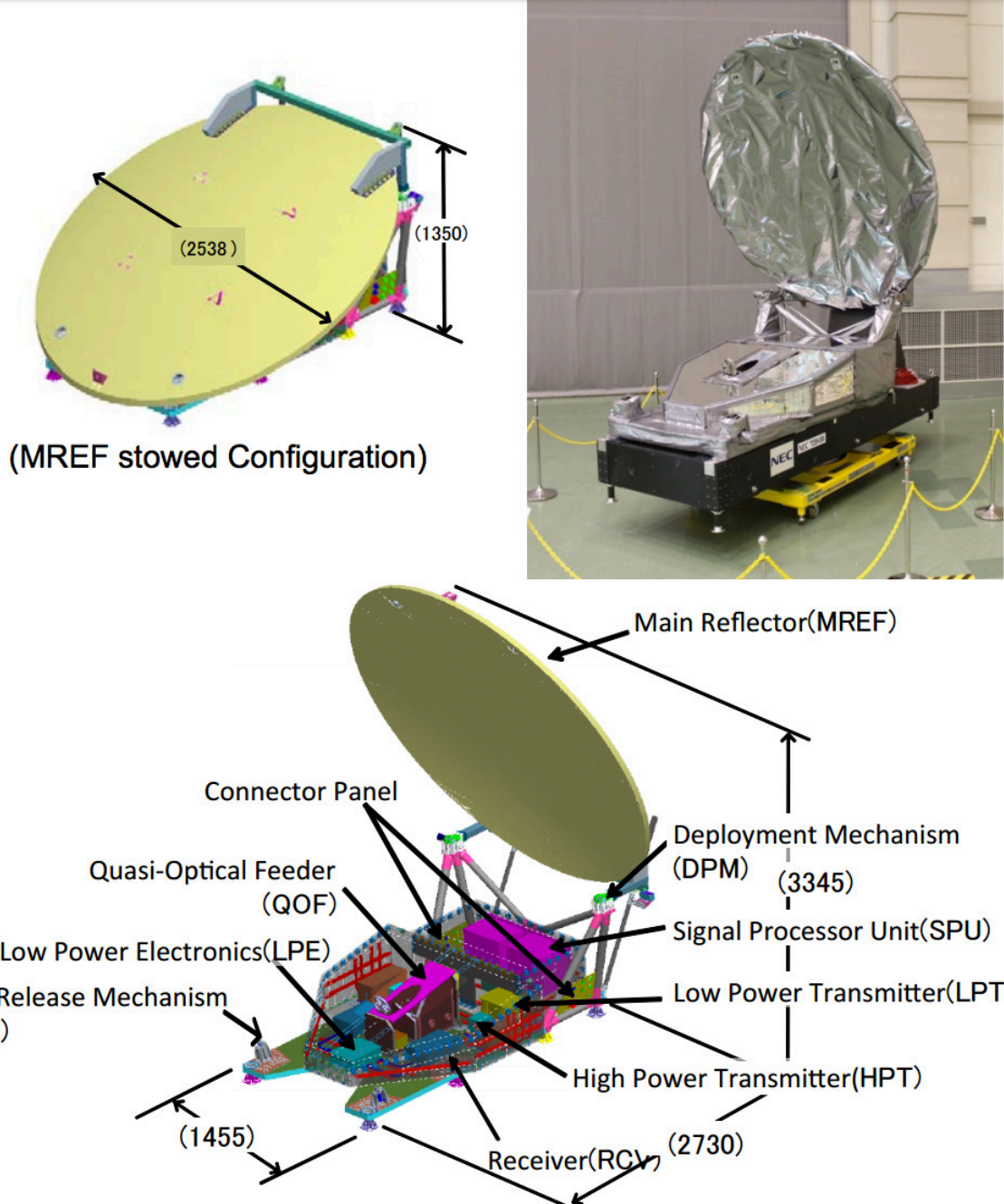


Figure 27: CPR in stowed and deployed configurations

A Transmit-Receive Subsystem encompasses the radar transmitter with its power supply and the receiver electronics. A quasi-optical feeder is used to emit the transmitter RF pulses towards the reflector and to collect the return signal for further on board processing. After down-conversion to IF frequency, the received signal is sent to the Signal Processing Unit (SPU). The SPU is also used as main CPR control unit and interface towards the spacecraft. Besides its high sensitivity, the CPR implements a unique Doppler capability that will allow it to retrieve the vertical velocity of the clouds particles.

1.4 The Multi Spectral Imager (MSI)

1.4.1 The MSI concept

MSI is a seven-band, push-broom scanner used to provide images at 500 m ground sampling distance over a 150 km wide swath, which is offset from nadir pointing and distributed -35 to +115 km in order to minimise sun-glint. The imagery will serve as context information for the quasi-simultaneous along track measurements of the CPR and ATLID, and also provide additional data on cloud types, texture, cloud top temperature and other micro-physical parameters such as cloud phase. Collection of aerosol information is a goal requirement. The level 1 product is radiance in the visible, near infrared (NIR) and short wave infrared (SWIR) bands, and brightness temperature in the thermal infrared (TIR) bands. The MSI channels approximate the wavebands of NOAA’s AVHRR with an additional TIR channel at 8.8 μm , common with the SEVIRI instrument on Meteosat Second Generation.

MSI consists of a separately accommodated 10 kg ICU and a 40 kg Optical Bench Module (OBM). The OBM comprises two cameras, one dedicated to the solar channels and one to the thermal infrared channels, both of which are mounted on the same optical bench and use a common Front End Electronics (FEE) unit. The FEE acquires and digitises the analogue signals generated by the optical detectors in response to the illumination from the Earth scene being observed. The ICU implements the routing of command and telemetry between the satellite and the instrument, as well as performing monitoring functions. It buffers data and assembles it with relevant house-keeping data into Instrument Source Packets.

The MSI development has been undertaken by SSTL, with the Visible/NIR/SWIR (VNS) module from TNO and the Instrument Control Unit (ICU) from TAS-UK.

	λ (μm)	$\Delta\lambda$ (μm)
Visible channel	0.67	0.02
NIR channel	0.865	0.02
SWIR1 channel	1.65	0.05
SWIR2 channel	2.21	0.10
TIR1 channel	8.8	0.9
TIR2 channel	10.8	0.9
TIR3 channel	12.0	0.9
Swath width	150 km	
Spatial sampling distance	500 m	
Spatial co-registration	0.15 SSD	
Radiometric accuracy	10 % or 1 K	
Inter channel accuracy	1 % or 0.25 K	
Radiometric stability	1 % or 0.3 K/year	

Table 5. Key performance parameters of MSI.

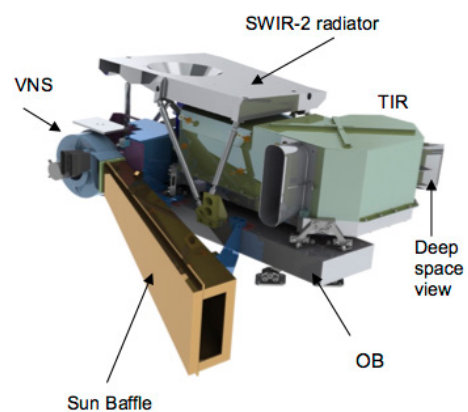


Figure 28. The MSI Optical Bench

	Low reference	SNR/NEDT	High reference	SNR/NEDT
Visible channel	30 W.m ⁻² .sr ⁻¹ . μm ⁻¹	75	444.6 W.m ⁻² .sr ⁻¹ . μm ⁻¹	500
NIR channel	17 W.m ⁻² .sr ⁻¹ . μm ⁻¹	65	282.7 W.m ⁻² .sr ⁻¹ . μm ⁻¹	500
SWIR1 channel	1.5 W.m ⁻² .sr ⁻¹ . μm ⁻¹	18	67.9 W.m ⁻² .sr ⁻¹ . μm ⁻¹	250
SWIR2 channel	0.5 W.m ⁻² .sr ⁻¹ . μm ⁻¹	21	24.6 W.m ⁻² .sr ⁻¹ . μm ⁻¹	250
TIR1 channel	220 K	0.80 K	293 K	0.25 K
TIR2 channel	220 K	0.80 K	293 K	0.25 K
TIR3 channel	220 K	0.80 K	293 K	0.25 K

Table 6. MSI reference dynamic range and required performance.

1.4.2 TIR camera module description

The TIR module uses a two part imaging system, consisting of a telescope and a relay, to focus the three channels onto a single area array detector. A rotating mirror allows the line of sight to be redirected onto an internal, warm blackbody and to deep space to perform a calibration once per orbit.

Optics: During imaging the Earth view is reflected by the calibration mirror onto a lens that forms the aperture. The fore optics forms an image of the scene at long focal length. The beam then enters the Filter and Dichroic Optical Components (FDOC) where it is split by two dichroic beam-splitters into three beams, which are reflected onto a common image plane and pass through their respective filters that define the response for each of the channels. The FDOC components are rectangular. There is an intermediate focus formed within the FDOC, allowing a field stop to be defined using the filters. The system is close to tele-centric in the region of the dichroics and filters. The filters are tilted up to 10° in order to control stray reflections, such that they all systematically reflect radiation from an internal reference inside the inner shroud (see Figure 7), thereby providing control of the out-of-band radiation directed by the filters to the detectors. In the fore optics temperature control in the order of 500 mK is adequate; at the detector, signal from this part of the structure and optics will be seen only in the subtended scene and via the filter transmission.

The beams enter the rear optics through three slots in a temperature-controlled plate. In the rear optics they are then re-imaged onto the microbolometer array with substantial de-magnification, with the final image at approximately f/1 with a ±11.3° field of view. The rear optics is contained in a thermally isolated enclosure, controlled in temperature to better than 100 mK.

The optics include Zinc Selenide, Germanium and Gallium Arsenide elements. Athermalisation is achieved by structural means; an Invar metering rod holds the detector in a position fixed with respect to the optics lens barrel over a 50° temperature range. The optic surface shapes include a number of aspherical components in order to be able to meet the imaging requirements. The optical system operates near the diffraction limit and it uses both oversampling and Time Delay Integration (TDI) to improve the signal to noise ratio (SNR).

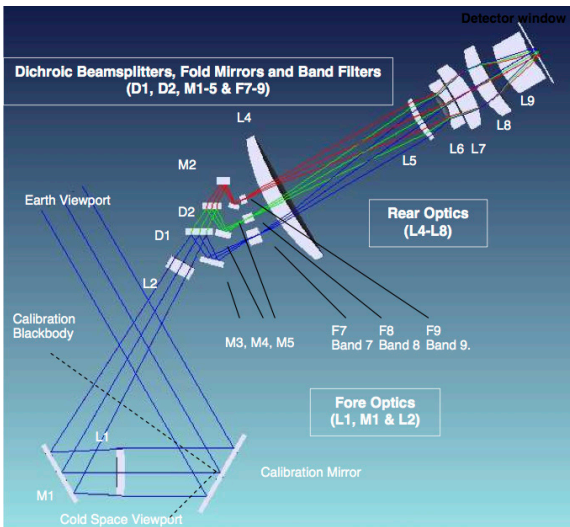


Figure 29. MSI TIR channel layout.

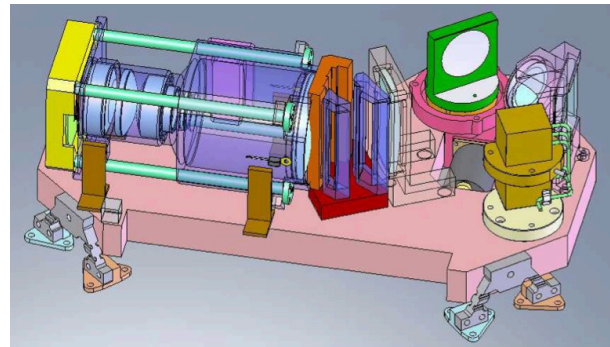


Figure 30. TIR inner shroud cut-away; Fore Optics to right of image, FDOC at centre, Relay Optics to left.

Detector: The detector is a ULIS microbolometer area array detector of 385x288 pixels at 35 μm pitch. The device is mounted in a flat package with an integral thermoelectric cooler (TEC) for thermal control.

Oversampling: the detector array can be read out several times per dwell period and the signal summed; this operation prevents overheating of the detector elements and increases SNR.

TDI: Signals from a predetermined number of rows (N) are co-added from N successive frames, which effectively multiplies the total ground signal from each ground pixel by the TDI factor, N. MSI TIR plans to use a TDI factor of 19, although the figure is adjustable on-orbit; the maximum TDI factor is 20, constrained by the width of the TIR spectral filters.

Reference area subtraction: Non-scene pixels, from reference blocks outside of the image area, can be used to measure signals due to background radiation from the lens relay structure and detector temperature drift. Subtraction of signals averaged over rows from reference image blocks will correct for short-term drifts (due detector & optics temperature drifts) and reduce the noise contributions that are correlated along rows and down columns.

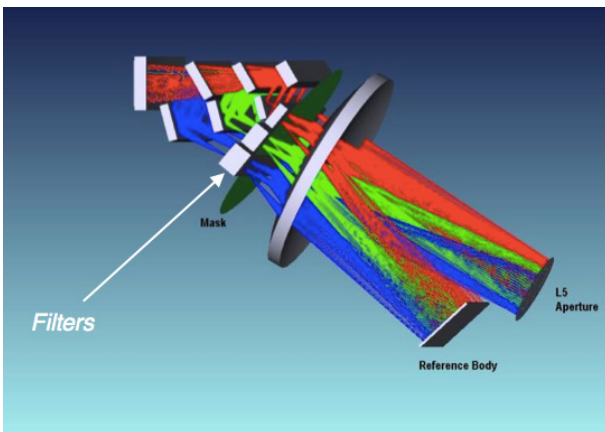


Figure 31. Reflection of radiation from internal reference.

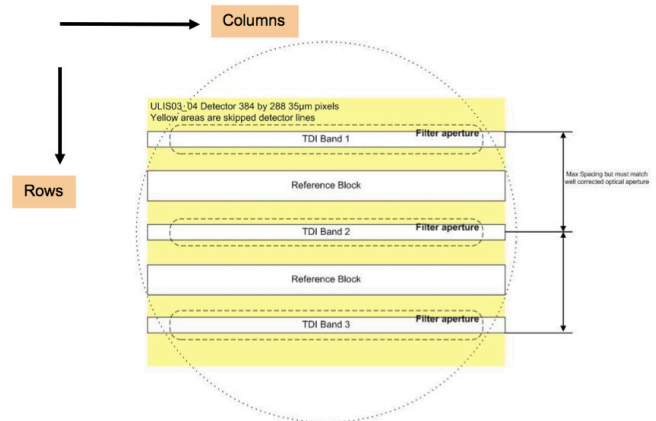


Figure 32. Microbolometer detector image and reference areas.

1.4.3 VNS camera module description

The VNS camera images light from the scene onto four different focal planes equipped with linear 512 photodiode arrays from XenICs, one focal plane for each channel. Bands VIS, NIR and SWIR-1 share a common 4.7 mm aperture

and are separated by a system of dichroics and beamsplitters. The SWIR-2 band has a larger, separate 10.4 mm aperture and the corresponding focal plane is stabilised at 235 K via a passive cooling system. The optical design accommodates the 25 μm pixels to provide an 11.5° field of view at f/4.58 for the VIS/NIR/SWIR1 channels and f/2.09 for SWIR2. The optical components include glasses such as NLaSF31, ZnS and Ge in the SWIR channels. A solar viewing port allows calibration of the four channels by detecting the solar light passed through a pair of diffusers placed in front of the aperture stop. The instrument aperture can be closed to calibrate the dark signal.

Whereas silicon detectors serve the VIS and NIR channels, the SWIR-1 channel is served by a standard InGaAs detector and the SWIR-2 channel by an extended wavelength InGaAs detector, offering better performance than MCT in high temperature operation. The diode arrays each incorporate two readout circuits, allowing odd/even redundancy to be used; use of the same read-out electronics for each detector array allows a single design to serve all four channels, simplifying the FEE. In a similar way to the TIR detector system, both oversampling (up to 64 times per line) and reference area subtraction is performed.

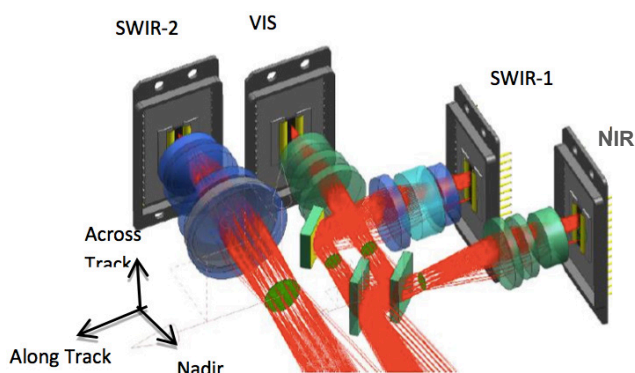


Figure 33. MSI VNS channel layout.

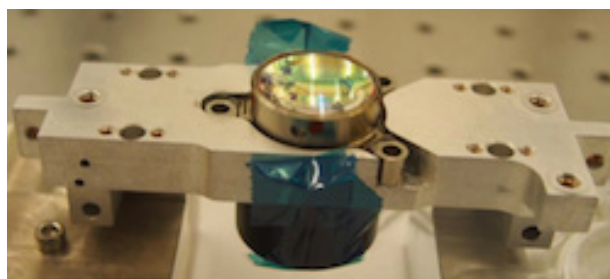


Figure 34. VIS channel barrel in its mount.

1.4.4 Calibration / Validation

The MSI response is linear and is calibrated using a high and a low radiance reference point. More detail on the calibration and performance of MSI is available.

TIR: The optics arrangement is designed such that the detectors receive radiation that is reflected from the filters and mounting frame, coming from a common, internal reference body, whose temperature tracks that of the structure and rear optics by means of a thermal link to the housing (see Figure 7). Signals from the reference areas will be averaged and subtracted from the signal in the scene area on the detector, allowing therefore to account for short term, relative temperature drifts. Absolute calibration is performed once per orbit against an internal, warm blackbody and by observation of deep space. The line of sight is redirected to the sources via an internal, rotating mirror. Prior to flight, the internal blackbody has been calibrated against an NIST traceable source from NPL. The space view will be calibrated using a source developed by SSTL.

VNS: The two radiance reference points for the VNS are 1) observation of solar light through a diffuser that can be rotated into the field of view and 2) instrument response with the aperture closed. Two pairs of Quasi Volume Diffusers (QVD) are carried, within each pair one for the SWIR2 and one for the other VNS channels. One QVD pair is routinely used once per orbit. The second pair is used approximately once per month, in order to monitor degradation of the nominal pair. The solar calibration is carried out in the South Polar Region, when the satellite has crossed the terminator and is flying over a shadowed earth, but still with the Sun in the line of sight. The dark calibration is performed on the dark side of the orbit.

1.4.5 MSI reconfiguration

Late during calibration of the VNS camera unexpected results led to the discovery that a thickness variance of the bandpass filter coatings, in each of the VIS, NIR and SWIR1 channels, was not meeting specification. The result was an across track variation (smile) in the spectral response (SR) that violated the instrument requirements.

For the worst affected channel, the NIR, a re-design was identified and implemented, with the bandpass filter applied to a flat surface, and manufacture of a new camera channel or objective undertaken. For the VIS channel, the existing barrel was removed, rotated 180° around its optical axis and re-mounted. The refurbished MSI expected performance is compatible with its primary mission objectives.

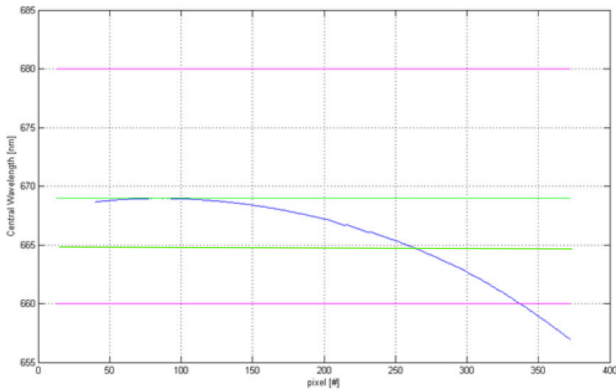


Figure 35. SR of VIS following barrel rotation; measured at barrel level. Pink lines indicate spectral channel width requirement and green lines indicate requirement on SR across the swath (smile).

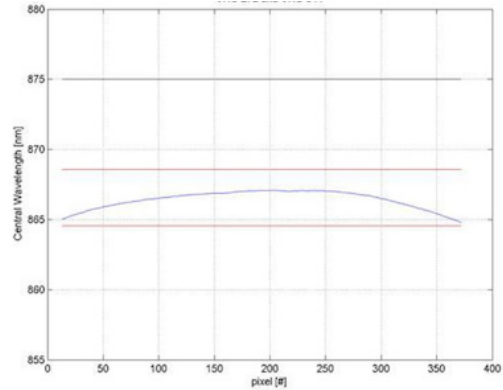


Figure 36. SR of NIR channel following redesign; measured at barrel level (pre integration of the barrel into the VNS unit).
The nadir pixel is at px 103

VNS flight model rebuild has been successfully completed and the full verification campaign, including environmental acceptance testing as well as calibration, has started in summer 2016.

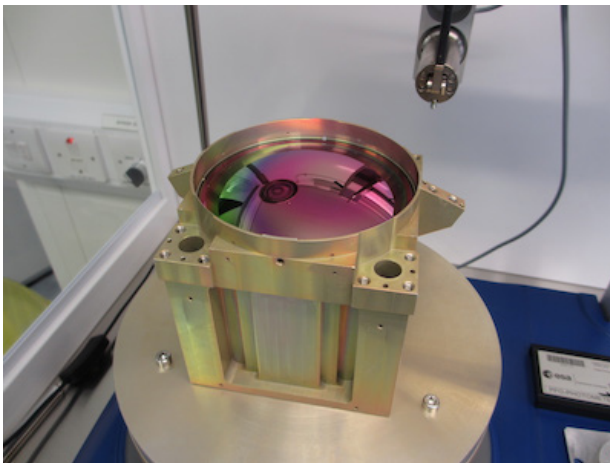


Figure 37. TIR flight relay lens.

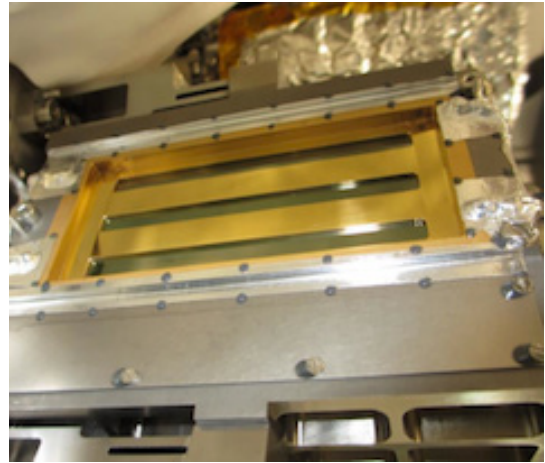


Figure 38. FDOC with gaps to structure closed with chofoil.

4. SUMMARY

The EarthCARE platform will provide simultaneous views from a Cloud Profiling Radar, an Atmospheric Lidar, a MultiSpectral Imager and a BroadBand Radiometer. Data products will be generated for both individual instruments and for common products, since the instruments can be used in a synergistic manner. The data acquired will be used to improve atmospheric models of cloud-aerosol interactions and understanding of their effect on the Earth radiation budget. The instruments of making up its payload have been presented. The EarthCARE launch is foreseen towards the end of 2019 and will be followed by a 6-month Cal/Val Phase that will precede a 30 Month routine operations phase.